Quantification of Lifeline System Interdependencies after the 27 February 2010 M_w 8.8 Offshore Maule, Chile, Earthquake

Leonardo Dueñas-Osorio,[a] **M.EERI, and Alexis Kwasinski**[b]

Data on lifeline system service restoration is seldom exploited for the calibration of performance prediction models or for response comparisons across systems and events. This study explores utility restoration curves after the 2010 Chilean earthquake through a time series method to quantify coupling strengths across lifeline systems. When consistent with field information, cross-correlations from restoration curves without significant lag times quantify operational interdependence, whereas those with significant lags reveal logistical interdependence. Synthesized coupling strengths are also proposed to incorporate cross-correlations and lag times at once. In the Chilean earthquake, coupling across fixed and mobile phones was the strongest per region followed by coupling within and across telecommunication and power systems in adjacent regions. Unapparent couplings were also revealed among telecommunication and power systems with water networks. The proposed methodology can steer new protocols for post-disaster data collection, including anecdotal information to evaluate causality, and inform infrastructure interdependence effect prediction models. [DOI: 10.1193/1.4000054]

INTRODUCTION

Available post-disaster restoration data from lifeline systems is seldom investigated statistically to find performance correlations or levels of interdependence. Conducting such data analyses while informed by anecdotal field information can provide the basis for quantifying and comparing interdependence across events while informing multi-infrastructure performance prediction models. Note that the existence of interdependence across utility systems is widely recognized (Rinaldi et al. 2001), but its quantification (coupling strength) is only starting to be formalized. Hence, this study uses available restoration data from power, potable water, and telecommunication systems, as well as field observations collected by the Technical Council on Lifeline Earthquake Engineering (TCLEE) after the 27 February 2010 M_w 8.8 Offshore Maule, Chile, earthquake, to introduce a practical time series approach for quantifying lifeline system interdependencies.

The complexity of modern lifeline systems has prompted a multidisciplinary effort to model and predict the performance of interacting systems under a variety of operating

[a] Assistant Professor, Department of Civil and Environmental Engineering, Rice University, Houston, TX 77005
[b] Assistant Professor, Department of Electrical and Computer Engineering, The University of Texas at Austin, Austin, TX 78712

Earthquake Spectra, Volume 28, No. S1, pages S581–S603, June 2012; © 2012, Earthquake Engineering Research Institute

conditions (Satumtira and Dueñas-Osorio 2010). Most research on interdependent infrastructures has focused on the modeling aspects, producing a rich set of flexible approaches that include agent-based programs (Rinaldi et al. 2001, Brown et al. 2004, Balducelli et al. 2005), input-output inoperability methods (Haimes and Jiang 2001, Santos and Haimes 2004, Barker and Haimes 2009), and more recently deterministic and stochastic graph theoretic approaches with different degrees of sophistication to capture connectivity and flow (Dueñas-Osorio et al. 2007a,b, Svendsen and Wolthusen 2007, Adachi and Ellingwood 2008, Rosato et al. 2008, Kim et al. 2009, Ouyang et al. 2009, Hernández-Fajardo and Dueñas-Osorio 2011, Ouyang and Dueñas-Osorio 2011). Although these modeling efforts enable scenario event and probabilistic risk analyses of interdependent lifeline systems, the lack of measured coupling strengths under diverse operating conditions is still a major contributor to the uncertainty of performance predictions that could be used for system planning, operation and design. A few exceptions of calibration of predictive lifeline performance models under natural hazards with interdependencies include Wang (2006), Bonneau and O'Rourke (2009) and Wu and Dueñas-Osorio (2012), among others.

Customarily, existing data to calibrate the coupling strength across infrastructure systems is obtained from normal operation conditions through economic input-output scores that link infrastructure sectors (Haimes et al. 2005). However, the coupling strength across infrastructure systems is not well understood after abnormal operation conditions, as triggered by earthquakes, hurricanes, internal failures, or deliberate attacks to name a few. Post-event coupling strengths may not only synthesize typical lifeline system *operational coupling*, related to the direct influence one system has on the functionality of others and vice versa through the supply and demand of commodities and information, but also capture the ability of infrastructure system operators to coordinate, deploy resources, and restore services once other systems are functional, referred in this work to as *logistical coupling*. Evidence of post-event coupling strengths in conjunction with anecdotal field data is increasing with time, while more empirical records are available from different disruptive events. Examples of this emerging data include the analysis of media reports on incidents that involve infrastructure system loss of functionality, along with associated frequency analyses to reveal relationships between triggering events and their consequences within and across systems. Other approaches rely on data released by local public utility commissions and utility providers in terms of restoration efforts. However, available post-event data and associated collection methodologies have been conditioned by the nature of the disruptive event as no standardized data collection methodologies for interdependent infrastructure have been widely adopted. However, current efforts by TCLEE are aiming at updating the protocols for post-disaster data collection to enable a standardized quantification of coupling strengths by different methods, including the new time series approach from this study.

Representative examples of post-event empirical coupling strengths across infrastructure systems have been spurred by acts of terrorism, particularly after the September 11, 2001 World Trade Center (WTC) attacks (Mendonca and Wallace 2006). Frequency and linear correlation analyses across networked infrastructure incidents and their impacts as reported by the media, and captured by Pearson's correlations (r), are used to quantify interdependence. The work by Mendonca and Wallace (2006) reports correlations from $r = 0.10$ to 0.19 between different lifeline systems (note that other metrics could be computed, including the

Spearman's and Kendall's correlations). Negative correlations have also been measured, particularly between service sectors and utility systems. Hence, correlations could be used to calibrate the strength of coupling across lifeline system models, although recent studies, without a frequency-based incident focus, also report valuable consequences of failure along with system interdependencies that are useful in model calibration (O'Rourke 2007).

Other empirical studies based on the frequency analysis of media-reported incidents to quantify interdependence have concentrated on the propagation of failures from the power grid to other systems under multiple natural hazard events (McDaniels et al. 2007, Chang et al. 2009). These studies present a systematic methodology to rank incidents and determine their joint extent and intensity. Consequence indices as well as ratios of intensity versus extent could also be used to calibrate interdependent infrastructure models and explore mitigation actions that control the consequences from different disruptive events.

Some empirical studies that do not rely on media reports of infrastructure incidents resort to data maintained by local public utility commissions and utility service providers (Park et al. 2006, Reed et al. 2009). The used data sets are desirable because they measure actual restoration processes in terms of customers served or other quality metrics. When studying the seismic or hurricane performance of power systems, the percentage of outages per number of customers per area, or the percentage of damaged network facilities per area, are typically used to generate fragility curves, which relate the probability of failure to hazard intensity levels. These empirically-based fragility relationships enable the performance and resilience evaluation of individual and coupled infrastructures given the occurrence of predefined disruptive scenarios, as well as the validation of theoretical and computational models of network interactions. However, these studies have not exploited the temporal nature of restoration evolution to quantify coupling strengths across distinct lifeline systems.

In contrast to a frequency analysis of incidents, along with their pair-wise correlations, or to frequency based fragility curves, this study exploits the time-evolving nature of suitable restoration curves to perform exploratory analyses in a time series context. Such analyses applied to the Chile earthquake data sets yield autocorrelations and cross-correlations among restoration curves of different lifeline systems, allow quantifying their strength of coupling, and permit establishing the leading or lagging characteristics of system response to seismic hazards at different geographical locations as a function of time—features difficult to achieve jointly with existing media- and resilience-based methods to quantify interdependence.

The remaining content of the paper is structured as follows. The next section briefly describes the types of data needed for a time series approach to quantifying interdependencies across utility systems. Then, some details of the 27 February 2010 M_w 8.8 Offshore Maule, Chile, earthquake, along with the triggered damage on utility systems are presented. Afterwards, the field collected time dependent restoration curves are introduced with basic descriptions of their characteristics. Then, the exploratory time series analyses take place, followed by an analysis of results in terms of coupling strength across lifeline systems. The paper ends with conclusions, potential mitigation efforts to cope with direct and interdependent lifeline system failure in practice, and insights for future research.

DATA REQUIREMENTS FOR INTERDEPENDENCE QUANTIFICATION

The quantification of coupling strengths across utility systems for the calibration of predictive models of system performance and support of maintenance and retrofit decisions can readily rely on the information encoded in time-dependent restoration curves, whose analysis is one of the goals of this study. Ideally, restoration data sets should be collected at different levels of geographical resolution and for most of the critical infrastructure systems, including electric power, telecommunications, water and wastewater, oil and gas, transportation, and services such as finance and banking (DHS 2003). Also, restoration curves, in terms of fractions of subscribers with service or satisfied demand, should be procured at fine time intervals to capture the evolution of recovery and facilitate statistical analyses, while enriched by anecdotal information. Given typical post-disaster conditions on the ground, restoration curves at the service area level of granularity should be the minimum aim (e.g., areas served by distribution substations in the power system, or analogous geographies for other lifeline systems). However, this poses unique requirements on utility providers, who typically compromise by sharing city, regional, or national-level service restoration data sets. Shared data often include the restoration of power, water and wastewater, oil and gas, telecommunication and transportation systems with status updates every 6 to 8 hours.

The information obtained by the TCLEE team in Chile was adequate, but, as with most post-earthquake investigations, not necessarily complete or suitable for a systematic experimental design. Also, the team obtained restoration curves with daily updates not at the service area level of resolution but at the city and regional levels, where regions correspond to the Chilean political division). However, the available data was deemed sufficient to explore common lifeline systems within and across two of the contiguous Chilean regions closest to the epicenter of the earthquake, and also for two major cities in each of these regions, where the cities represent coastal and inland communities per region. In particular, regional level power and telecommunication restoration curves were secured, along with power recovery at each of the two cities per region, and the potable water restoration for the major cities of one of the regions (all introduced in subsequent sections).

Despite the collected information not representing and ideal dataset in geographical extent and diversity of infrastructure systems, it still provides enough material to perform mathematical analyses to quantify the strength of coupling across lifeline systems and confirm relationships with field anecdotal accounts, while uncovering unexpected trends difficult to visualize or measure otherwise. The time series analyses for strength of coupling quantification are performed across all pairs of lifeline systems per region and among similar systems across regions. Some details of the Chilean earthquake are first summarized to provide the necessary context for lifeline system interdependence assessments.

BASICS OF THE M_W 8.8 OFFSHORE MAULE, CHILE, EARTHQUAKE

The M_w 8.8 offshore Maule earthquake occurred in central Chile on February 27, 2010 at 3:34 AM local time (06:34 UTC). This event, called the "Cauquenes" earthquake by the National Seismological Service (SSN for its acronym in Spanish) of the University of Chile, exhibited a rupture area with approximately 450 km in length by 125 km in width (Figure 1). Displacements in the rupture zone exceeded 10 m, which translated into permanent displacements of up to 3.0 m horizontally (westbound) and 1.1 m vertically (upwards) in

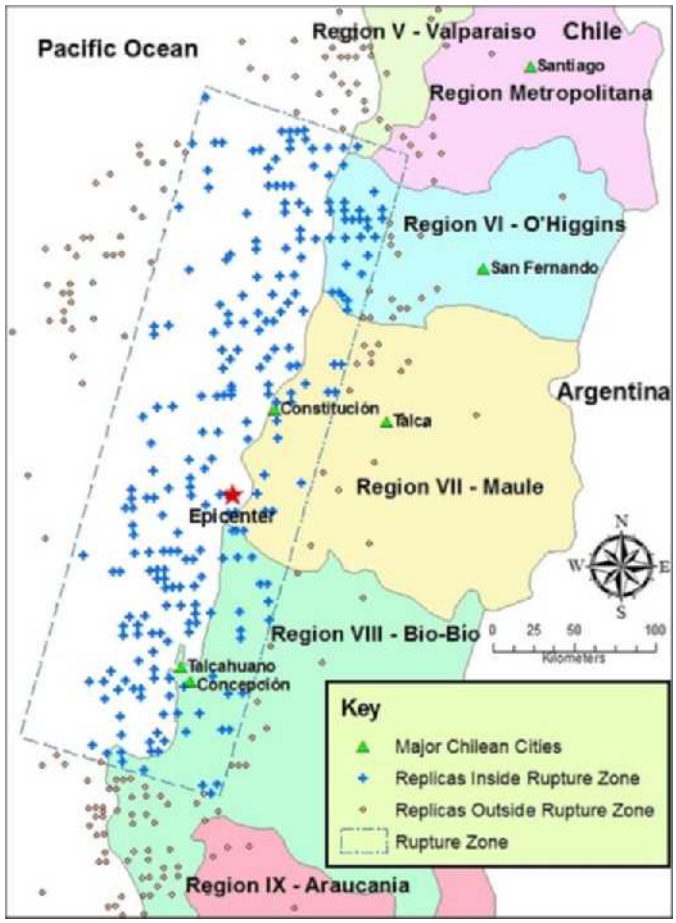

Figure 1. Location of the rupture initiation with approximate area of displacement between the Nazca and South American Plates. Nearly 65% of the replicas with $M_w > 4.7$ as of May 2010 occurred inside this rupture area between Chilean Regions VI and VIII. Adapted from Barrientos (2010).

the city of Concepción (Ruegg et al. 2009, UNAVCO 2010, USGS 2010). Concepción is the second largest urban area after the capital Santiago de Chile, with close to 1,000,000 inhabitants and located 105 km south-southwest of the epicenter.

Regarding peak ground accelerations (PGA), the top five values recorded by the Chilean SSN exceeded 0.30 g, with one of the highest levels recorded at bedrock in the city of Concepción with a PGA $\geq$ 0.6 g in the two orthogonal horizontal and vertical directions (Universidad de Chile 2010). The USGS instrumental intensity data, which correspond to estimates of Modified Mercalli Intensity (MMI) levels as a function of field reports and recorded peak accelerations and velocities, matched perceived shaking by residents of Concepción and Talcahuano, who anecdotally described the event as "very strong" to "violent."

The earthquake also produced a tsunami that caused major damage in coastal cities along 500 km of coastline. One of the hardest hit cities was Constitución in Region VII, where wave heights ranged from 6.9 m to 11.2 m. The city of Talcahuano in Region VIII, which is just northwest of Concepción, was also heavily affected by the tsunami, although the wave heights were lower than in Constitución in the range of 3.3 m to 6.3 m (EERI 2010).

EARTHQUAKE EFFECTS ON INTERDEPENDENT LIFELINE SYSTEMS

Direct earthquake damage to lifeline systems in Regions VI through VIII ranged from sporadic failures in the power systems to widespread failures in the water and gas systems. Also, direct damage revealed component design weaknesses and inadequate back-up systems in the transportation and telecommunication systems, respectively. Details and photographs documenting critical lifeline system performance are available from the TCLEE post-earthquake investigation report (TCLEE 2010). A monograph with extended and reviewed material on the Chile earthquake is expected to be published by the end of 2012. However, a short description of the response of individual and interdependent systems is provided below.

The power transmission and distribution systems responded relatively well to earthquake demands by exhibiting overall minor to moderate damage. Most power at the transmission level was restored within 24 hours of the event, while most of the power at the sub-transmission level was available after 72 hours. However, there were avoidable delays caused in part by telecommunication system unavailability and congestion, a shortage of back-up generators and fuel for internal communications, and public unrest. Generation loss was minimal and its impact minor as demand was reduced. At the distribution level, physical damage was observed due to collapsed facades and structures on power lines, but it was not widespread (Araneda et al. 2010)—except in coastal areas. Most power restoration at the distribution level (< 13.3 kV) took up to two weeks.

Telecommunication service providers, both landline and wireless, experienced setbacks due to congestion, commercial power outages, equipment failures, building and structure failures, loss of energy storage, and lack of reserve power in most distributed network facilities. Failures at indoor cell sites were mainly due to unanchored battery racks and other operational equipment. Although only a handful of towers collapsed, fallen and misaligned antennae from towers were another common occurrence. Cellular communications equipment on top of damaged structures was also compromised at multiple locations. With the exception of large and medium capacity central offices, almost all communication sites lacked permanent standby generators. In addition, portable backup power was difficult to buy or rent while the theft of equipment contributed to restoration delays. Most cellular phone service providers restored their services to the majority of users within two weeks.

The urban potable water system in Concepción and Talcahuano was severely damaged, mainly due to soil failure and damaged buried pipes of a wide range of diameters. Breaks and leaks were more frequent on small diameter pipes, although several large diameter steel pipes were also damaged. Water treatment plants were mainly affected structurally at the water intake sites and clarifiers, as well as non-structurally at the control and water quality control rooms. The restoration of water and waste water systems was also delayed in the first few days after the event, in part due to the lack of communications and street violence.

Regarding the transportation network, it had a barely acceptable performance that allowed for crucial post-earthquake recovery efforts to take place, despite the collapse of bridges and overpasses. Bridges rendered non-functional after the earthquake tended to have inadequate support length and restraints, weak shear connections, deficient foundations to handle soil liquefaction, and soil slumping at access ramps. Alternate routes and bailey bridges enabled the flow of goods across the affected areas, but at the expense of lengthier travel times, restricted flow, and uncertainty about the distribution of critical commodities. Road connectivity was mostly reestablished with limited capacity within 24 hours.

OBSERVED LIFELINE SYSTEM INTERDEPENDENCIES

Infrastructure interdependence between power, transportation, telecommunication and water systems contributed to the loss of functionality and delayed restoration processes. The extra functionality loss was due to physical and operational interactions between lifeline systems, and from specific cases of collocation. Also, interdependencies affected regional resilience, or the ability to rapidly restore service. Although interdependence acts a contributor to functionality loss, coupling across systems is important during normal operation for the optimal use of systems (Min and Dueñas-Osorio 2010, Ouyang and Dueñas-Osorio 2011).

Regarding field observations, post-event operational interdependence was very strong during the early phase after the earthquake, which was characterized by uncertainty about road network conditions, the absence of power, telecommunications, water, and other services, along with public turmoil. This phase had different durations, but for the Concepción area it lasted approximately three days. During this time, there were blackouts at the power transmission and sub-transmission levels, affecting telecommunication systems. The water infrastructure had adequate emergency power to operate treatment plants in emergency mode, although there was high uncertainty on fuel availability. In addition, the lack of telecommunications delayed early hiring as well as coordination and assignment of water system crews to field repairs. Lack of telecommunications during the blackout phase also led to delays in assessing the damage and safety of power distribution systems.

The following phase, 72 hours after the event and with most power transmission restored, was characterized by the increasing availability of alternate transportation routes, restoration of power at the sub-transmission and distribution levels, and re-established social order. These factors enabled a steady recovery of telecommunications (despite initial congestion) and more efficient repairs in water and gas networks. Infrastructure performance recovery after the blackout phase also led to a reduction in operational interdependence while increasing logistical interdependence and indirect losses at focused locations—a trend also observed in non-seismic disasters (Mendonca and Wallace 2006, Chang et al. 2009).

Although, underground, overhead, and surface level infrastructure collocation cases provided additional mechanisms for interaction, only a few triggered failures. Examples included telecommunication, gas, and water lines conveyed by collapsed or excessively displaced bridges at waterway crossings or quay walls at port facilities, as well as electric train halts from power and telecommunication downed poles, rooftop telecommunication structure failures or cut operations at collapsed or tagged for demolition buildings, and power distribution lines pulled down from collapsed housing facades or structures.

Collocation factors as well as operational and logistical interdependencies during and after the blackout phases could all be reasonably captured by lifeline system restoration curves. These recovery time series and their cross-correlations synthesize resilience and coupling strengths when analyzed in light of field observations and anecdotal accounts.

AVAILABLE LIFELINE SYSTEM RESTORATION CURVES

Lifeline system restoration data was obtained from the TCLEE team, from the Ministry of the Interior of the Chilean government, and reports from utility companies in Regions VI through VIII, including the water and wastewater company ESSBIO and the power transmission and distribution company CGE. Specifically, data on the percentage of customer service availability as a function of time was obtained for power and water distribution in the cities of Concepción and Talcahuano, which represent inland and coastal communities in Region VIII, respectively. Also, average restoration curves for Regions VII and VIII were obtained for power and telecommunications (fixed and mobile telephones). Power restoration data was also collected for the cities of Talca and Constitución, representing inland and coastal communities in Region VII, respectively. Regions and cities are displayed in Figure 1.

Recovery progress is typically reported by discounting permanently lost customers, mainly from coastal areas affected by the tsunami, as it shows higher levels of accomplishment (Araneda et al. 2010). Figure 2 presents the available average data on lifeline system recovery for Region VIII. Note that although longer time or higher resolution plots are desirable, the shared data by utility providers was only synthesized daily for approximately two weeks. However, these curves still show the different global trends between utilities. For

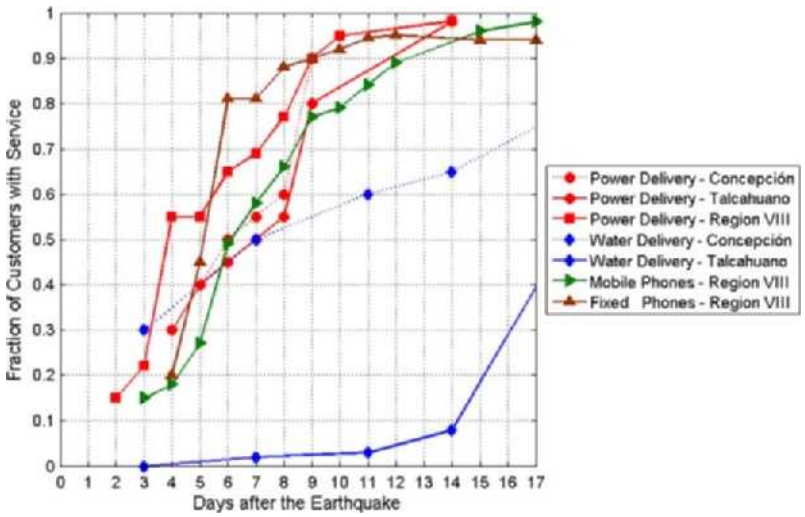

Figure 2. Service restoration time series for available utility systems in select cities and across the Bío-Bío Region VIII. Note that the fraction of customers per service right after the earthquake was unknown; only after the second day official restoration fractions started to be available.

instance, integrating the equalized restoration curves between days 0 to 17, and normalizing the results by the time of integration, a measure of resilience is obtained (Reed et al. 2009). This resilience or normalized customer-days of service availability provides relative comparisons across lifeline systems and regions, and even across distinct disruptive events, as it takes values between desirable $R = 1.0$ and undesirable $R = 0$. The first column with numerical values in Table 1 shows the quantified resilience. For comparison with other recent disasters, the earthquake resilience of the power systems in Regions VII and VIII was $R \geq 0.70$, while the power system resilience in the state of Louisiana in the United States after 17 days of Hurricane Katrina's landfall was $R = 0.54$, capturing the higher level of devastation caused by the storm surge, inundation, and wind speeds of such a destructive hurricane.

Specific to Region VIII, there is a higher availability of power across the Region than mobile and fixed phone service. Also, power restoration in Concepción and Talcahuano tends to be higher relative to mobile telecommunication systems in the entire Region. These trends and the relatively small differences in resilience of the noted examples suggest a tight operational interaction between power and communication systems as seen in Figure 2 and as recalled by utility operators. Also, note the higher availability of landlines relative to mobile phones over the entire restoration phase, a fact exploited by most other utility companies to organize their logistics via fixed telephones. In practice, central offices with more than 5,000 subscribers typically had adequate backup power generation and although congested, most never lost service. Finally, the evident direct seismic damage on the water distribution system overshadowed any visible interdependent effects on water system operation or restoration from the coupling with power, telecommunications or fuel transportation. However, as shown in the next section, time series analyses of restoration curves can uncover some of the field-reported logistical interdependencies between water and other systems—details not captured by visual inspection of the curves or by aggregate metrics such as R.

Table 1. Basic statistical analysis of available lifeline system restoration curves

	Restoration Curves	Resilience (R)	j^{th} Identifier	Entire Series				
				m_j	σ_j	ρ_j (1)	ρ_j (2)	$\Delta\rho$ (%)
Region VIII	Fixed Phones Region VIII	0.66	F_VIII	−0.002	0.285	−0.253	−0.150	40.65
	Mobile Phones Region VIII	0.59	M_VIII	−0.026	0.409	−0.283	−0.277	2.08
	Power Delivery Region VIII	0.70	P_VIII	−0.013	0.330	−0.628	0.211	133.53
	Power Delivery Concepción	0.65	P_C_VIII	0.000	0.412	−0.436	−0.041	90.49
	Power Delivery Talcahuano	0.62	P_T_VIII	−0.017	0.338	−0.431	−0.008	98.16
	Water Delivery Concepción	0.49	W_C_VIII	−0.184	0.300	0.385	0.243	37.03
	Water Delivery Talcahuano	0.05	W_T_VIII	−0.001	0.269	−0.061	−0.195	216.94
Region VII	Fixed Phones Region VII	0.75	F_VII	−0.004	0.329	−0.543	0.254	146.74
	Mobile Phones Region VII	0.69	M_VII	−0.004	0.424	−0.692	0.490	170.90
	Power Delivery Region VII	0.73	P_VII	−0.017	0.340	−0.603	0.122	120.32
	Power Delivery Constitución	0.67	P_C_VII	−0.025	0.357	−0.467	0.105	122.53
	Power Delivery Talca	0.76	P_T_VII	−0.071	0.394	−0.603	0.414	168.62

Figure 3 presents the available service restoration curves for Region VII. The restoration trends for power and telecommunication systems are similar to Region VIII, although recovery in Region VII was faster, as confirmed by *R*. The figure also shows a gap between the power restoration of coastal and inland cities (Constitución and Talca, respectively), given the severe damage in the tsunami area. This gap is not observed in Region VIII because Concepción and Talcahuano are geographically adjacent and tsunami effects were more contained. Additionally, Constitución showed a higher percentage of collapsed or severely damaged buildings than in the other cities due to its proximity to the earthquake epicenter and the higher percentage of adobe buildings. The damage and permanent loss of customers in Constitución also played a role in making its restoration slightly faster than in coastal Talcahuano. In addition, the drop in fixed phone services starting in day 12 was more pronounced in region VII as weakened facades were further damaged, taking with them restored fixed phone lines, following a major M_w 6.9 aftershock on 11 March 2010. Central offices also experienced further damage and associated congestion, while buildings and homes tagged for demolition were being removed along with their restored fixed lines.

The time evolving nature of the restoration curves allows a natural exploration of the data in time series contexts. These analyses permit quantification of the leading or lagging relations in the data, reveal hidden restoration trends, and provide an alternative and practical way to measure interdependence strength across lifeline systems. Note that traditional Pearson correlations, if computed, yield high values across all pairs of restoration curves as all curves tend to increase with time. In fact, the average correlation across all pairs is approximately 0.88, reflecting the high value of pair-wise correlations, but also that such correlations are not able to capture lagging or leading trends across the restoration processes of different systems, as the time series approach of this research does.

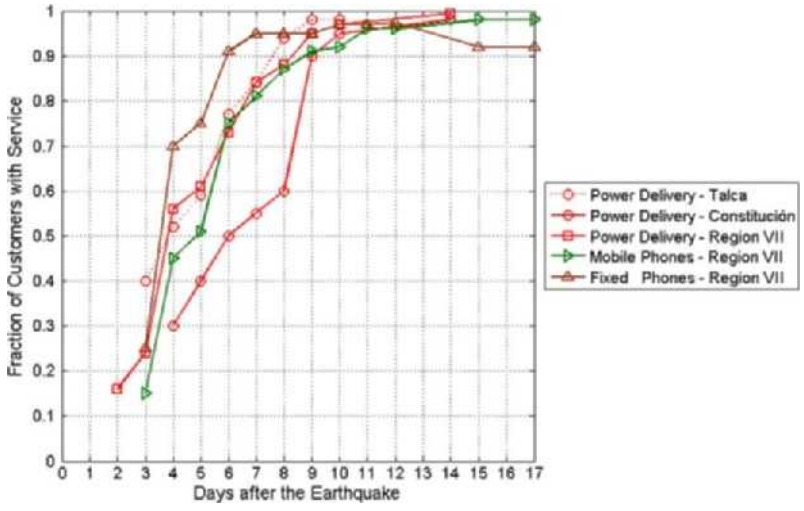

Figure 3. Restoration time series for available utility systems across the Maule Region VII.

TIME SERIES ANALYSES FOR INTERDEPENDENCE QUANTIFICATION

To perform exploratory analyses of data series in the time domain, it is desirable that the data be at least weakly stationary (Shumway and Stoffer 2006). However, it is difficult to achieve this condition for short time series such as the restoration curves in Figures 2 and 3. To minimize the effects of nonstationarity and obtain meaningful statistical analyses, the authors have logarithmically transformed and second-differenced the time series to at least achieve weak stationarity. This transformation attempts to stabilize variability, reach constancy of the mean μ_t of the time series at times t (i.e., $\mu_t = \mu = m$, so that it does not depend on time t), and achieve auto-covariance values that decay rapidly and only depend on the time-difference $h = t_1 - t_2$ between the series, where t_1 and t_2 are arbitrary points in time (Shumway and Stoffer 2006).

Before transforming and differencing the time series, the length of the vectors containing the restoration data for the different utility systems is equalized. Figures 2 and 3 show that all series have data from days 4 to 14, while some start in days 2 or 3, or end in day 17. Hence, length equalization requires extrapolating some series from day 14 to day 17, which is deemed adequate as they are close to 100% restoration by day 14. Also, all series are initiated at day 0 by extrapolating their trend depending on the utility system under consideration. These first few days of extrapolated restoration process are assumed as representative of the early recovery from complete outage given that no actual records exist. Private communications between the authors and service providers support this assumption for mobile networks, which had under 10% of coverage 36 hours after the earthquake (relative to 15% after the first 72 hours when the restoration curves start). The sample means of the equalized, transformed and differenced restoration curves are evaluated as follows:

$$\bar{x}_j = m_j = \frac{1}{1 + n_j} \sum_{t=0}^{n_j} x_{t,j} \tag{1}$$

where $x_{t,j}$ is the t^{th} value of the j^{th} differenced restoration curve, $t = 0,\ 1, \ldots, n_j$, and n_j is the time of the last observation for each of the transformed restoration series—in this study $n_j = 17$ for all j. This sample mean per time series becomes handy to numerically assess another metric that quantifies the degree of linear correlation between adjacent restoration curve values $x_{t,j}$ and $x_{t+h,j}$ across all feasible t. This quantity is referred to as the autocorrelation, which is computed as a function of the autocovariance in Equation 2. It measures the similarity between individual observations of the restoration curves as a function of the time separation between them, where high values represent high degree of linear dependence (from smooth restoration series) and low values represent independence (from series with sharp contrasts). Note that dependencies, if present, do not necessarily mean causation, but simply point out to similarities in adjacent values and associated trends which may or may not be explained in terms of field anecdotal data. However, as presented in the following section, many of the trends and insights from the statistical analyzes align with field observations and implemented restoration processes. The autocorrelation functions (ACF) in Equation 3 correspond to the normalized version of the autocovariance functions in Equation 2, which are preferable for dimensionless comparisons.

$$\widehat{\gamma}_j(h) = \frac{1}{1+n_j}\sum_{t=0}^{n_j-h}(x_{t+h,j}-\bar{x}_j)(x_{t,j}-\bar{x}_j) \tag{2}$$

$$\rho_j(h) = \frac{\widehat{\gamma}_j(h)}{\widehat{\gamma}_j(0)} \tag{3}$$

A more pertinent metric to quantify the strength of restoration coupling across lifeline systems is the cross-correlation function (CCF). This is a normalized version of the cross-covariance function and a tool to analyze the joint behavior between different time series—a task yet to be performed in lifeline system engineering. For two transformed restoration curves j and k with series $x_{t,j}$ and $x_{t,k}$, their sample cross-covariance is provided in Equation 4 and their cross-correlation in Equation 5, which can be measured for different lag times h. Hence, the CCF values can measure in practice the predictability of one series, say $x_{t,j}$ as a function of another series $x_{t,k}$ for a given lag time h between them, where high CCF values (close to 1.0) represent high predictability. In the context of interdependence analyses, CCF values and associated h levels can measure the strength of coupling between lifeline systems or how the restoration process of one system predicts the restoration of another one, although without necessarily imputing causation, which can be evaluated against field logs in the examination of results phase. Typically, the sample cross-correlations are also explored graphically as function of the lag time h to easily search for leading or lagging relations across series, as well as for comparisons of significant peaks to reveal coupling strengths.

$$\widehat{\gamma}_{j,k}(h) = \frac{1}{1+n_j}\sum_{t=0}^{n_j-h}(x_{t+h,j}-\bar{x}_j)(x_{t,k}-\bar{x}_k) \tag{4}$$

$$\rho_{j,k}(h) = \frac{\widehat{\gamma}_{j,k}(h)}{\sqrt{\widehat{\gamma}_j(0)\widehat{\gamma}_k(0)}} \tag{5}$$

APPLICATION OF TIME SERIES ANALYSES TO RESTORATION CURVES

Table 1 lists the 12 restoration curves used in this study along with their j^{th} identifier, and reports data about their mean m_j, standard deviation σ_j, and autocorrelations ρ_j with their percent differences $\Delta\rho$ when evaluated at two h values. Hence, besides the resilience values per time series, this table has the necessary information to assess their levels of stationarity and dependence.

The table shows that the mean values of the transformed and differenced series tend to zero, their standard deviations are high, and the change between autocorrelations at lag times $h = 1$ and 2, or $\rho(1)$ and $\rho(2)$, are high—all desirable features suggesting stationarity to support autocorrelation and cross-correlation analyses. In particular, these observations are suggestive of *weakly* stationary behavior, although due to the shortness of the series some remain non-stationary. Time series lengths are expected to improve from new protocols by TCLEE for data collection at higher sampling rates during post-earthquake investigations.

For the restoration curves at hand, Figure 4 presents a sample of two series for the city of Concepción with contrasting behavior, along with their $\rho_j(h)$ values (labeled as ACFs in the bottom of each figure part) for all possible lag times h. Sharp cut offs or quick decays in the ACF values of Figure 4a provide evidence of weak stationarity; the top of Figure 4a simply shows the transformed and differenced version of the restoration curve. In contrast, Figure 4b

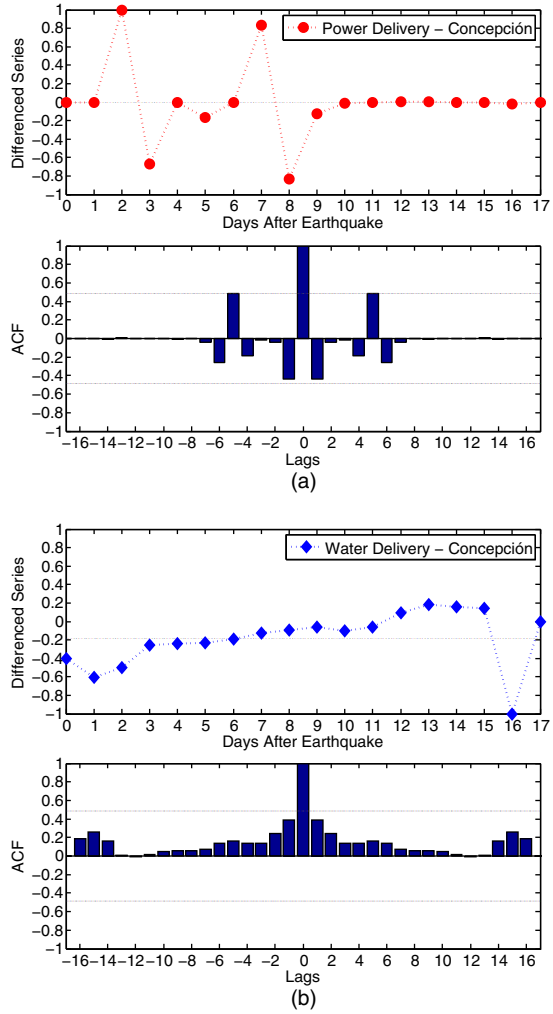

Figure 4. Auto-correlation function values for multiple lags h of two series with distinct stationary behavior in Concepción. (a) Power delivery in Concepción, Region VIII: Evidence of weakly stationary behavior. (b) Water delivery in Concepción, Region VIII: Traces of nonstationarity. The horizontal line in the differenced series parts represents the mean value of the series, while the horizontal lines in the ACF parts indicate the threshold for statistical significance of the peaks in large samples.

shows a slow decay of ACF values and some trends in the transformed restoration curve, indicating traces of nonstationarity, which require interpretation of these particular results with caution. However, the practical meaning of a series with slow decays in the ACF values across h levels is that the restoration process is steady and somewhat predictable. Note that the maximum ACF = 1.0 occurs when $h = 0$ indicating how the time series relates to itself, while for other values of h, it indicates how the time series relates to the same signal but lagged or led by h units of time. A slow decay of ACF levels aligns with the restoration pattern for the water system in Concepción, as its recovery was very slow due to heavy physical damage, but progress from one day to the next was comparable. The sharply changing ACF values of the power system shown in Figure 4a suggests that the restoration progress in one day had little to do with the recovery trend on the next day, mainly because with power systems, restoration was addressed based on not just transmission lines and main feeders, but also laterals and distribution system level equipment, which is less predictable.

The ACF plots for most other non-water system series, not shown here, reveal that they behave like Figure 4a, even in the few cases when the difference between autocorrelations at lags $h = 1$ and 2 is small (Table 1). This is because relative to the lag $h = 0$, there is a sharp decay in $\rho_j(h)$. Also, note that Table 1 uncovers a regional effect in which the ACF values are more contrasting in Region VII than in Region VIII, due to the faster restoration in Region VII. In addition, most time series had initial speed ups in restoration as in Figure 4a, which tended to repeat between two to six days after the earthquake as evidenced by positive ACF spikes of different magnitude, some significant, except for water systems. These spikes reflect field conditions where crews accelerated restoration tasks after a few days following the earthquake given better information and logistics. Clearly, the water system was the exception, although field repair work effects manifest as restored service with delays in cross-correlation analyses, which are at the core of subsequent lifeline coupling assessments.

QUANTIFICATION OF THE STRENGTH OF COUPLING

The CCFs, particularly the positive values, capture the degree of correlation across different lifeline system restoration curves, which permit the quantification of interdependencies. Sample CCFs versus lag times h are presented in Figure 5 for several series with distinct coupling strengths. Figure 5a shows two restoration curves with high CCF at a small positive lag time of $h = 2$, where the positive sign indicates that the fixed phone restoration lags relative to the power restoration. This relation was only hinted in Figure 2, but explicit here. The small value of h also suggests that the two systems affect each other's operation, where power outages and recovery affected telecommunication systems accordingly. Figure 5b shows two restoration curves with weak correlation at a high negative lag time of $h = -8$, indicating that power delivery in Concepción had a tendency to lead, albeit indirectly due to high negative h, the restoration of water delivery. This is due to the heavy direct damage of water pipelines. Hence, cross-correlation effects at high h levels indicate not operational but logistical coupling, where the coordination of repair crews and equipment from power availability materialized several days later in terms of water system service restoration.

To fully explore cross-correlations, Table 2 presents a summary of the peak CCF values for all restoration curve pairs in Region VIII along with their lag values h. As with fixed

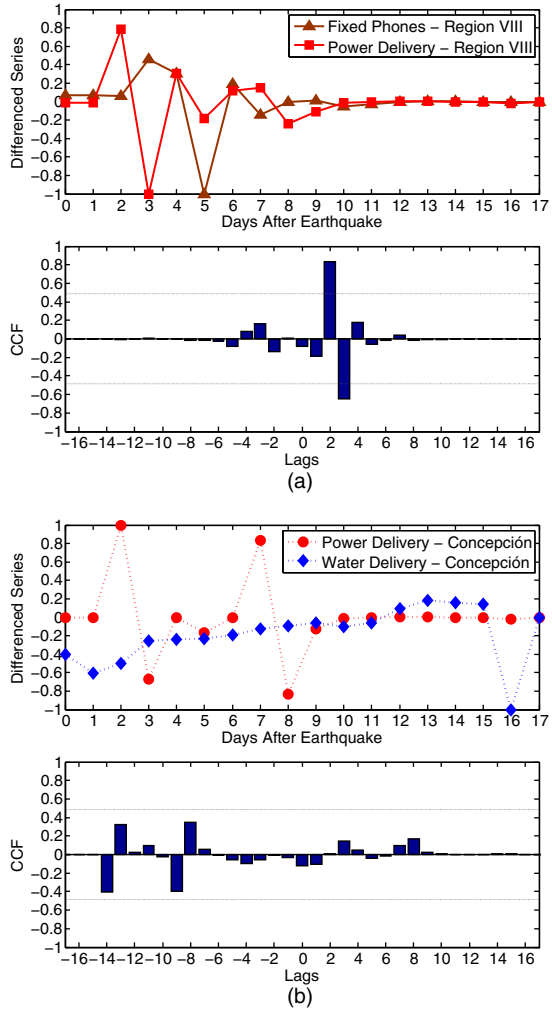

Figure 5. Cross-correlation function values for multiple lags h for two pairs of series with distinct coupling strengths. (a) Strong correlation between fixed phones and power in Region VIII. (b) Weak correlation between power and water delivery in Concepción.

phones, mobile phones also have a high correlation with regional power delivery at $h = 2$, indicating operational interdependence in agreement with TCLEE team observations. Interestingly, regional power and telecommunications, along with local power, have a high correlation with water delivery but with high negative lag times, highlighting water system logistical dependence on other utilities. Fixed and mobile phones also exhibit high correlation at no lag time as these two systems share infrastructure, as does the water system in adjacent inland and coastal cities. Power in Concepción leads the recovery of power in Talcahuano by almost a week, possibly due to the tsunami effects in the coastal city. Also, power at the

Table 2. Symmetric cross-correlation and lag values for restoration curves in Region VIII. Gray areas represent high CCF values ≥ 60% and bold fonts represent CCF values ≥ 80%. Systems in the rows lead (lag) the systems in the columns when the h values are negative (positive).

	F_VIII		M_VIII		P_VIII		P_C_VIII		P_T_VIII		W_C_VIII		W_T_VIII	
Series	Peak ρ	Lag h	Peak ρ	Lag h	Peak ρ	Lag h	Peak ρ	Lag h	Peak ρ	Lag h	Peak ρ	Lag h	Peak ρ	Lag h
F_VIII	1.00	0.00	0.74	0.00	**0.84**	2.00	0.53	2.00	0.74	−3.00	0.66	−11.00	**0.96**	−11.00
M_VIII	0.74	0.00	1.00	0.00	0.73	2.00	0.64	2.00	**0.83**	−3.00	0.48	−11.00	0.74	−11.00
P_VIII	**0.84**	−2.00	0.73	−2.00	1.00	0.00	0.79	0.00	**0.89**	−5.00	0.56	−13.00	0.79	−13.00
P_C_VIII	0.53	−2.00	0.64	−2.00	0.79	0.00	1.00	0.00	0.68	−5.00	0.35	−8.00	0.53	−8.00
P_T_VIII	0.74	3.00	**0.83**	3.00	**0.89**	5.00	0.68	5.00	1.00	0.00	0.50	−8.00	0.75	−8.00
W_C_VIII	0.66	11.00	0.48	11.00	0.56	13.00	0.35	8.00	0.50	8.00	1.00	0.00	0.70	0.00
W_T_VIII	**0.96**	11.00	0.74	11.00	0.79	13.00	0.53	8.00	0.75	8.00	0.70	0.00	1.00	0.00

regional level leads coastal city restorations or interacts instantaneously with inland city restorations, which aligns with reality, as the inland cities tend to be the largest per region.

Correlation levels in the less damaged Region VII are higher than in region VIII due to tighter operational dependence (Table 3), supporting causal relationships reported in the field. For example, fixed phone restorations are highly correlated to mobile phone and regional power delivery recovery at no lag times, given less physical damage and strong operational coupling via shared infrastructure. Note the strong correlations between fixed telephone lines and both regional and local power delivery as well as the also high correlations between mobile phones and power. Correlation between power and fixed telephony is expected because at the distribution level both networks share the power distribution infrastructure, thus highlighting causal relationships. High correlation between power and mobile communication systems is also expected because the shortage of fixed and portable generators led to cell site outages that were only operational after commercial power restoration. These observations support the visual trends and field data in Figure 3 where fixed phones supported overall restoration activities. Correlation between power delivery across inland and

Table 3. Symmetric cross-correlation and lag values for restoration curves in Region VII

	F_VII		M_VII		P_VII		P_C_VII		P_T_VII	
Series	Peak ρ	Lag h	Peak ρ	Lag h	Peak ρ	Lag h	Peak ρ	Lag h	Peak ρ	Lag h
F_VII	1.00	0.00	**0.91**	0.00	**0.94**	0.00	**0.96**	−4.00	**0.89**	−2.00
M_VII	**0.91**	0.00	1.00	0.00	**0.83**	0.00	**0.88**	−4.00	**0.85**	−2.00
P_VII	**0.94**	0.00	**0.83**	0.00	1.00	0.00	**0.94**	−4.00	**0.89**	−2.00
P_C_VII	**0.96**	4.00	**0.88**	4.00	**0.94**	4.00	1.00	0.00	**0.88**	2.00
P_T_VII	**0.89**	2.00	**0.85**	2.00	**0.89**	2.00	**0.88**	−2.00	1.00	0.00

Table 4. Asymmetric cross-correlation and lag values for restorations across Regions VII and VIII.

	F_VIII		M_VIII		P_VIII		P_C_VIII		P_T_VIII	
Series	Peak ρ	Lag h	Peak ρ	Lag h	Peak ρ	Lag h	Peak ρ	Lag h	Peak ρ	Lag h
F_VII	**0.88**	−2.00	0.79	−2.00	**0.94**	0.00	0.64	0.00	**0.91**	−5.00
M_VII	0.78	−2.00	0.57	−2.00	**0.87**	0.00	0.58	0.00	0.75	−5.00
P_VII	**0.81**	−2.00	**0.87**	−2.00	**0.95**	0.00	0.76	0.00	**0.92**	−5.00
P_C_VII	**0.83**	2.00	**0.81**	2.00	**0.94**	4.00	0.68	4.00	**0.95**	−1.00
P_T_VII	0.63	0.00	0.68	0.00	**0.86**	2.00	0.63	2.00	**0.85**	−3.00

coastal cities is high with inland recovery leading the process, while regional power leads local power restoration as observed in the field and also in Region VIII.

The correlations across Regions VII and VIII can also be explored with the CCF methodology as presented in Table 4. Recovery of telecommunication systems and power in Region VII either led by $h = -2$ or had an immediate effect on the recovery of phones and regional or local power in Region VIII. This is due to the availability of essential lifeline systems in interconnected adjacent regions, which highlights the relevance of jurisdictional cooperation.

DISCUSSION AND OVERALL COUPLING STRENGTHS ACROSS LIFELINE SYSTEMS

In an attempt to synthesize the information contained in the CCF values and lag times h, this study quantifies the strength of coupling $S_{j,k}$ across lifeline systems by combining these two pieces of information. The parameter $S_{j,k}$ captures the recovery correlations between systems j and k while adjusting them as a function of peak lag times h—essentially transforming operational and logistical interdependences into equivalent system interdependencies. This synthesized coupling strength notion is consistent with actual observations where high h at peak CCF values indicate weak operational coupling, but still recognize the logistical interdependence of repair coordination. A simple yet realistic mathematical relation that captures the decay in interdependence as a function of h is the following overall coupling strength:

$$S_{j,k} = \begin{cases} \dfrac{-\rho^{+}_{j,k}(h)}{1 + \sqrt{|h|}} \times \mathrm{sgn}(h) & \text{when } h \neq 0 \\ \rho^{+}_{j,k}(h) & \text{when } h = 0 \end{cases} \tag{6}$$

where the cross-correlation value in the numerator $\rho^{+}_{j,k}$ corresponds to the maximum positive CCF value, which occurs at the peak lag time value h with absolute value $|h|$, and the sign function (sgn) is used to keep track of the dominant system in practice (where the jth system leads [lags] the restoration of the kth system when $S_{j,k}$ is positive [negative]). The functional form of Equation (6) for $h \neq 0$ recognizes a decaying trend in daily correlation across systems

as a function of time that agrees with field observations in that it balances the strength of the operational interdependence with the observed logistical interdependence, so as to be of general applicability in future post-earthquake reconnaissance missions. If h is measured in the field in units different from days, it needs to be transformed into day-equivalents. Note that the maximum $S_{j,k} = 1.0$ occurs when two systems are perfectly correlated at $h = 0$.

A summary of the overall coupling strengths that account for cross-correlations and lag effects across lifeline systems and regions is presented in Tables 5 through 7. The results

Table 5. Overall infrastructure coupling strengths in Region VIII. Gray areas represent coupling strength values ≥ 60% and bold fonts represent coupling values ≥ 80%. Systems in the rows lead (lag) the systems in the columns when the S values are positive (negative).

	F_VIII	M_VIII	P_VIII	P_C_VIII	P_T_VIII	W_C_VIII	W_T_VIII
Series				S			
F_VIII	1.00	0.74	−0.35	−0.22	0.27	0.15	0.22
M_VIII	0.74	1.00	−0.30	−0.27	0.30	0.11	0.17
P_VIII	0.35	0.30	1.00	0.79	0.28	0.12	0.17
P_C_VIII	0.22	0.27	0.79	1.00	0.21	0.09	0.14
P_T_VIII	−0.27	−0.30	−0.28	−0.21	1.00	0.13	0.20
W_C_VIII	−0.15	−0.11	−0.12	−0.09	−0.13	1.00	0.70
W_T_VIII	−0.22	−0.17	−0.17	−0.14	−0.20	0.70	1.00

Table 6. Infrastructure coupling strengths in Region VII

	F_VII	M_VII	P_VII	P_C_VII	P_T_VII
Series			S		
F_VII	1.00	**0.91**	**0.94**	0.32	0.37
M_VII	**0.91**	1.00	**0.83**	0.29	0.35
P_VII	**0.94**	**0.83**	1.00	0.31	0.37
P_C_VII	−0.32	−0.29	−0.31	1.00	−0.36
P_T_VII	−0.37	−0.35	−0.37	0.36	1.00

Table 7. Infrastructure coupling strengths across Regions VII and VIII

	F_VIII	M_VIII	P_VIII	P_C_VIII	P_T_VIII
Series			S		
F_VII	0.36	0.33	**0.94**	0.64	0.28
M_VII	0.32	0.24	**0.87**	0.58	0.23
P_VII	0.34	0.36	**0.95**	0.76	0.28
P_C_VII	−0.34	−0.34	−0.31	−0.23	0.47
P_T_VII	0.63	0.68	−0.36	−0.26	0.31

reveal important interdependencies between distinct telecommunication systems, and with power systems at the regional level, especially in Region VII where damage was not as widespread. Also, from the analysis of results across regions, Region VII utilities exhibit a high coupling with regional power in Region VIII due to their coordinated management and cross-border coupling, which agrees with national-level restoration processes, with regions to the north of Region VIII recovering at a fast rate. Note that the regional effects across lifeline systems are stronger than the local effects across them. The tables also highlight realistic coupling strengths across systems with low interdependence, such as the operational dependence of water networks in Region VIII being low yet still capturing their logistical dependence, and the high coupling across water systems themselves.

The information on coupling strengths is expected to inform predictive models of infrastructure interdependence under seismic hazards. This time series approach also has the potential to capture time-varying coupling strengths for future enhanced modeling. Note that interdependencies between the discussed utility networks and transportation systems were not studied here, providing an additional opportunity for future research on coupled lifeline systems.

CONCLUSIONS AND FUTURE WORK

This study provides a time-series approach and a new formulation to quantify the strength of coupling across lifeline systems by using restoration curves from several utilities after the 27 February 2010 M_w 8.8 Offshore Maule, Chile, earthquake. Such an approach exploits the nature of time-dependent restoration curves, and creates an alternative avenue to empirically assess infrastructure interdependence while utilizing operator anecdotal information on coupling across lifeline systems. Results from this work show that interdependencies are not negligible. In fact, a key insight from cross-correlation analyses of restoration time series along with their lag or lead time effects includes the relevance of telephone systems, both fixed and mobile, to their own operation and to the operation of power delivery systems and vice versa. Also, lifeline systems across adjacent geographical areas (e.g., Chilean Regions) show strong interdependence. This is especially true with telecommunication and power systems in one region with moderate damage leading the restoration of an adjacent region with extensive damage. Intra-dependence is also observed through couplings within systems of the same kind but studied at different jurisdictional sizes, particularly when regional restorations lead local recovery or inland cities lead coastal restoration. In addition, at the city level, power delivery shows logistical coupling with the restoration of water systems, a fact not clearly conveyed by raw restoration curves. Other regional utilities also show important logistical correlation with water systems, given significant lag times. Quantitative analyses of interdependence for other past or future events should also be pursued to identify event-specific and generalizable coupling trends across interconnected lifeline systems.

The entire set of assessed overall coupling strengths across lifeline systems could be used to inform computational and theoretical predictive models of infrastructure interdependence effects. In fact, this and other empirically-based coupling strength assessments can be used to perform coupling quantification cross-checking, and to calibrate and validate emerging techniques that evaluate interaction effects using input-output, agent-based models, and network science models, among others. Also, the proposed coupling strength quantification method could be extended for non-stationary or complex evolution of interdependence cases, including their spatial variations.

The availability of coupling strengths can also focus infrastructure mitigation and post-disaster restoration efforts by identifying highly interdependent systems. For instance, independent and high coverage radio systems can substitute telephone systems during emergencies and enhance the recovery coordination of power, water and other utility systems at the transmission and especially at the distribution level. Some of these emergency radio systems have been proposed in the past worldwide. However, cost requirements and power issues have limited their deployment. The use of satellite-based telephone service has also shown its effectiveness in the United States, particularly after recent hurricanes. However, satellite phone service could be affected during periods of high solar activity, as exemplified by difficulties in using satellite systems by electric utility crews when an unusually strong solar flare occurred a few weeks after Hurricane Katrina. Strengthening of commercial and public radio-stations can also enable the broadcasting of messages for repair crews and contractors to learn about meeting points with utility operators. Although this is a controversial method due to crews' security and operational effectiveness, the Region VIII water company ESSBIO in Chile relied on this method to initiate repair logistics before power restoration and during the early, congested periods of mobile and fixed phone operation. Diverse power supply at communication sites through distributed generation is also desirable. In cell sites with low power consumption, the use of alternative power, such as photovoltaic and wind generators could be an effective decoupling solution. Call congestion issues can be addressed by call priority programs as implemented in the United States by the National Communications System. Although this study did not consider transportation networks, their adequate performance, redundancy, and availability of short detours at critical locations can reduce the restoration times of lifelines and decrease the effects of socio-technical interdependent effects (Rokneddin et al. 2012).

Coupling examples that go beyond operational interdependence include logistical linkages with detrimental effects. For instance, banks in dense urban areas that were able to rapidly complete internal retrofit projects were not able to receive power and other utility services before demolition of neighboring tagged buildings. Such demolition and re-installation of utility infrastructure process can represent business interruption for at least 4 to 6 months after the earthquake. Also, as the rate of restoration of most of the different lifeline systems slows down after the majority of their customers are back on line, the remaining residential and commercial users can endure inconvenience and indirect losses from lifeline system dependence, delayed recovery of the local economy, and decreased international trade. To ameliorate some of the long-term interdependence effects, decentralized availability of emergency water and gas tanks can mitigate delays in restoration. Also, the use of high-density polyethylene (HDPE) in certain main water distribution pipes demonstrated outstanding performance at the limited locations where it was used, which can reduce the lengthy restoration times of buried pipelines. These practical approaches and their effects could be de-aggregated from restoration curves, especially if collected at small geographical levels of resolution and if sampled at high time rates, so as to better understand triggers of speed ups and identify causes of slowdowns in restoration activities across lifeline systems.

ACKNOWLEDGMENTS

The present work was funded in part by the National Science Foundation through grants CMMI-0748231 and ECCS-0845828. The authors would also like to thank the Technical Council on Lifeline Earthquake Engineering (TCLEE) and its earthquake investigation

team. The group included team leader A. Tang, along with 10 other investigators listed alphabetically: T. Cooper, L. Dueñas-Osorio, J. Eidinger, B. Fullerton, R. Imbsen, L. Kempner Jr., A. Kwasinski, A. Pyrch, A. Schiff, and Y. Wang. The authors also acknowledge the support from the Universidad de la Santísima Concepción through professor Mauricio Villagrán, and the Pontificia Universidad Católica de Chile through professor Hugh Rudnick. In addition, the authors acknowledge support from ESSBIO, the water and waste water company in the Region, and the Compañia General de Electricidad (CGE). Finally, the authors would like to thank J. Rutenberg at Rice University for the time series analysis codes.

REFERENCES

Adachi, T., and Ellingwood, B., 2008. Serviceability of earthquake-damaged water systems: Effects of electrical power availability and power backup systems on system vulnerability, *Reliability Engineering and System Safety* **93**, 78–88.

Araneda, J. C., Rudnick, H., Mocarquer, S., and Miquel, P., 2010. Lessons from the 2010 Chilean earthquake and its impact on electric supply, *Proceedings of the 2010 International Conference on Power Systems Technology* (*Powercon* 2010), Hangzhou, China, 24–28 October 2010.

Balducelli, C., Bologna, S., Di Pietro, A., and Vicolo, G., 2005. Analysing interdependencies of critical infrastructures using agent discrete event simulation. *Int. J. of Emerg. Management* **2**, 306–318.

Barrientos, S., 2010. Terremoto Cauquenes 27 Febrero 2010, Informe Técnico Actualizado a Mayo 27 de 2010, *Servicio Sismológico*, Departamento de Geofisica, Universidad de Chile, http://www.sismologia.cl/informes/INFORME_TECNICO.pdf (accessed June 2010).

Barker, K., and Haimes, Y., 2009. Assessing uncertainty in extreme events: Applications to risk-based decision making in interdependent infrastructure sectors, *Rel. Eng. and Syst. Saf.* **94**, 819–829.

Bonneau, A., and O'Rourke, T. D., 2009. Water Supply Performance During Earthquakes and Extreme Events, Report No. MCEER-03 0009, MCEER, University at Buffalo, Buffalo, NY.

Brown, T., Beyeler, W., and Barton, D., 2004. Assessing infrastructure interdependencies: The challenge of risk analysis for complex adaptive systems, *Int. J. of Crit. Infrast.* **1**, 108–117.

Chang, S., McDaniels, T., and Beaubien, C., 2009. Societal impacts of infrastructure failure interdependencies: building an empirical knowledge based, *Proc. of the 2009 TCLEE Conference*, Oakland, CA, 28 June–1 July 2009, 693–702.

Dueñas-Osorio, L., Craig, J. I., and Goodno, B. J., 2007a. Seismic response of critical interdependent networks, *Earthquake Engineering and Structural Dynamics* **36**, 285–306.

Dueñas-Osorio, L., Craig, J. I., Goodno, B. J., and Bostrom, A., 2007b. Interdependent response of networked systems, *Journal of Infrastructure Systems* **13**, 185–194.

Earthquake Engineering Research Institute (EERI), 2010. The M_w 8.8 Chile earthquake of February 27, 2010, Learning from Earthquakes Special Report, *EERI Newsletter* **44**, Insert 1–20. http://www.eeri.org/site/images/eeri_newsletter/2010_pdf/Chile10_insert.pdf.

Haimes, Y. Y., and Jiang, P., 2001. Leontief-Based Model of Risk in Complex Interconnected Infrastructures, *ASCE Journal of Infrastructure Systems* **7**, 1–12.

Haimes, Y. Y., Horowitz, B. M., Lambert, J. H., Santos, J. R., Lian, C., and Crowther, K. G., 2005. Inoperability input-output model for interdependent infrastructure sectors. I: Theory and methodology, *ASCE Journal of Infrastructure Systems* **11**, 67–79.

Hernández, I., and Dueñas-Osorio, L., 2011. Time sequential response evolution of interdependent lifeline systems, *Earthquake Spectra* **27**, 23–43.

Institute for Electrical and Electronics Engineers (IEEE), 2005. *IEEE Recommended Practice for Seismic Design of Substations*, IEEE Standard 693, IEEE Power Engineering Society.

Kim, Y., Spencer, B., Elnashai, A., and Song, J., 2009. Seismic performance assessment of interdependent lifeline systems, *International Journal of Engineering under Uncertainty: Hazards, Assessment, and Mitigation* **1**, 173–181.

McDaniels, T., Chang, S., Peterson, K., Mikawoz, J., and Reed, D., 2007. Empirical framework for characterizing infrastructure failure interdependencies, *Journal of Infrast. Systems* **13**, 175–184.

Mendonca, D., and Wallace, W. A., 2006. Impacts of the 2001 World Trade Center attack on New York City critical infrastructures, *ASCE Journal of Infrastructure Systems* **12**, 260–270.

Min, X., and Dueñas-Osorio, L., 2010. Design of interdependent interfaces for lifeline systems using response surface inverse reliability methods, *Proceedings of the 9th U.S. National and 10th Canadian Conference on Earthquake Engineering*, Toronto, Canada, 25–29 July 2010.

O'Rourke, T., 2007. Critical infrastructure, interdependencies and resilience, *The Bridge* **37**, 22–29.

Ouyang, M., and Dueñas-Osorio, L., 2011. An approach to design interface topologies across interdependent urban infrastructure systems, *Reliability Eng. and Syst. Safety* **96**, 1462–1473.

Ouyang, M., Hong, L., Zijun, M., Ming-Hui, Y., and Fei, Q., 2009. A methodological approach to analyze vulnerability of interdependent infrastructures, *Sim. Mod. Pract. and Theory* **17**, 817–828.

Park, J., Nojima, N., and Reed, D., 2006. Nisqually earthquake electric utility analysis, *Earthquake Spectra* **22**, 491–509.

Reed, D., Kapur, K., and Christie, R. D., 2009. Methodology for assessing the resilience of networked infrastructure, *IEEE Systems Journal* **3**, 174–180.

Rinaldi, S., Peerenboom, J., and Kelly, T., 2001. Identifying, understanding, and analyzing critical infrastructures interdependencies, *IEEE Control Systems Magazine* **21**, 11–25.

Rokneddin, K., Ghosh, J., Dueñas–Osorio, L., and Padgett, J. E., 2011. Bridge retrofit prioritization for aging transportation networks subject to seismic hazards, *Structure and Infrastructure Engineering*, doi: 10.1080/15732479.2011.654230.

Rosato, V., Tiriticco, F., Issacharof, L., De Porcellinis, S., and Setola, R., 2008. Modeling interdependent infrastructures using interacting dynamical models, *Int. J. of Crit. Inf.* **4**, 63–79.

Ruegg, J., Rudloff, A., Vigny, C., Madariaga, R., de Chabalier, J., Campos, J., Kausel, E., Barrientos, S., and Dimitrov, D., 2009. Interseismic strain accumulation measured by GPS in the seismic gap between Constitución and Concepción in Chile, *Phys. of the Earth and Plan. Int.* **175**, 78–85.

Santos, J. R., and Haimes, Y. Y., 2004. Modeling the demand reduction input-output (I-O) inoperability due to terrorism of interconnected infrastructures, *Risk Analysis* **24**, 1437–1451.

Satumtira, G., and Dueñas-Osorio, L., 2010. Synthesis of modeling and simulation methods on critical infrastructure interdependencies research, in *Sustainable Infrastructure Systems: Simulation, Imaging, and Intelligent Engineering*, Gopalakrishnan, K., and Peeta, S. (Eds.), Springer, New York, 300 pp.

Shumway, R. H., and Stoffer, D. S., 2006. *Time Series Analysis and Its Applications*, Springer, New York, 596 pp.

Svendsen, N., and Wolthusen, S., 2007. Connectivity models of interdependency in mixed-type critical infrastructure networks, *Information Security Technical Report* **12**, 44–55.

Technical Council on Lifeline Earthquake Engineering (TCLEE), 2010. Preliminary report on lifeline system performance after the M_w 8.8 offshore Maule, Chile, earthquake of February 27, 2010, *American Society of Civil Engineers (ASCE)*, http://www.asce.org/uploadedFiles/Institutes/Technical_Activities_Committees_(TAC)/TCLEE%20Chile%20Web%20Report%207.10.pdf (accessed July 2010).

Universidad de Chile, 2010. Informe de últimos sismos sensibles, *Servicio Sismológico, Departamento de Geofísica, Universidad de Chile*, http://www.sismologia.cl (accessed June 2010).

University NAVSTAR Consortium (UNAVCO), 2010. Science Highlights 2010 - UNAVCO Event Response – M_w 8.8 Chile Earthquake February 27, 2010. *UNAVCO Research and Science*, http://www.unavco.org/research_science/science_highlights/2010/M8.8-Chile.html (June 2010).

U.S. Department of Homeland Security (DHS), 2003. *The National Strategy for the Physical Protection of Critical Infrastructures and Key Assets*, Government Printing Office, Washington D.C.

U.S. Geological Survey (USGS), 2010. *Magnitude 8.8–Offshore Maule, Chile*, Earthquake Hazards Program, http://earthquake.usgs.gov/earthquakes/eqinthenews/2010/us2010tfan.

Wang, Y., 2006. Seismic Performance Evaluation of Water Supply Systems, Ph.D. Thesis, Cornell University.

Wu, J., and Dueñas-Osorio, L., 2012. Calibration and validation of a seismic damage propagation model for interdependent infrastructure systems, *Earthquake Spectra*, in press.

(Received 4 August 2010; accepted 7 July 2012)